Journal of Power Sources 188 (2009) 458–462

Contents lists available at ScienceDirect

Journal of Power Sources

journal homepage: www.elsevier.com/locate/jpowsour

Short communication

The study of Au/MoS_2 anode catalyst for solid oxide fuel cell (SOFC) using H_2S-containing syngas fuel

Zheng-Rong Xu, Jing-Li Luo*, Karl T. Chuang

Department of Chemical and Materials Engineering, University of Alberta, Edmonton, AB, Canada T6G 2G6

ARTICLE INFO

Article history:
Received 31 October 2008
Received in revised form
29 November 2008
Accepted 1 December 2008
Available online 7 December 2008

Keywords:
Synthesis gas (syngas)
Au
MoS_2
Hydrogen sulfide (H_2S)
SOFC

ABSTRACT

Au/MoS_2 is a promising anode catalyst for conversion of all components of H_2S-containing syngas in solid oxide fuel cell (SOFC). MoS_2-supported nano-Au particles have catalytic activity for conversion of CO when syngas is used as fuel in SOFC systems, thus preventing poisoning of MoS_2 active sites by CO. In contrast to use of MoS_2 as anode catalyst, performance of Au/MoS_2 anode catalyst improves when CO is present in the feed. Current density over 600 mA cm^{-2} and maximum power density over 70 mW cm^{-2} were obtained at 900 °C, showing that Au/MoS_2 could be potentially used as sulfur-tolerant catalyst in fuel cell applications.

1. Introduction

Large amounts of synthesis gas (syngas) are produced worldwide each year by reforming different kinds of hydrocarbon resources, primarily for use in production of hydrogen, as reactant to produce petrochemicals, and as fuel for electrical power plants. Recently interest has grown in use of syngas for fuel cell applications. Solid oxide fuel cells (SOFCs) can provide higher energy conversion efficiency when compared with conventional power generation, and SOFCs can operate on a variety of fuels. One proposed application is using synthesis gas as fuel in the SOFCs. The major combustible components of syngas are H_2 and CO, which will take the following reactions (Eqs. (1) and (2)):

$$H_2 + (1/2)O_2 = H_2O \quad (1)$$

$$CO + (1/2)O_2 = CO_2 \quad (2)$$

When hydrocarbon resources are converted to syngas the sulfur and nitrogen content of the resource are also converted, and CO could react further to generate CO_2. Thus, raw syngas typically is a mixture of which the major components are H_2 and CO contaminated with CO_2, H_2S and nitrogen compounds. Table 1 shows the composition of syngas from different companies [1]. H_2S is commonly present, at concentrations ranging from several hundred ppm level to several thousand ppm. In SOFC systems, H_2S is corrosive to structural components and poisons most of the commonly used anode catalysts, such as Ni and Pt [2,3]. Consequently, an external sulfur removal step is required to remove virtually all H_2S from SOFC feeds for commercial fuel cell systems [4].

It is extremely expensive to remove virtually all H_2S from conventional fuel cell feeds, thus fuel purification adversely affects fuel cell economics. To improve cost efficiency, it is more attractive to directly use H_2S-containing syngas in SOFC systems. In past years, several related research projects have attempted [5–7]. H_2S-free syngas and H_2S-containing H_2 have been investigated as fuels for SOFC [8–10]. It has been shown that pure H_2S can be used as fuel in SOFC [11,12]. However, very little attention has been paid to use of H_2S-containing syngas as fuel in SOFCs. To do so, it is crucial to find a catalyst which is stable in a H_2S-rich environment and also has good catalytic activity for conversion of H_2 and CO. To this end we now describe syngas fuel cells having a new Au/MoS_2 anode catalyst.

Metal sulfides are widely used as catalysts for industrial applications [13,14]. Among them, MoS_2 and its derivatives are commonly used catalysts for desulphurization of hydrocarbons and other processes [15–17]. MoS_2 has a high melting point and good stability in H_2S-rich environments [18,19]. Bulk MoS_2 normally has a consolidated laminar structure. Finely divided MoS_2 catalysts have been developed having porous structure and high surface area [20–22]. Its applications as anode catalyst in SOFC were studied using both pure and diluted H_2S feeds. MoS_2 showed good catalytic activity for the conversion of H_2 and H_2S in SOFCs; however, it showed poor activity for the conversion of CO [11,12,23].

Supported gold catalyst has been reported to have high CO oxidation activity [24,25]. Gold catalysts supported on various support,

* Corresponding author. Tel.: +1 780 492 2232.
E-mail address: jingli.luo@ualberta.ca (J.-L. Luo).

0378-7753/$ – see front matter © 2008 Elsevier B.V. All rights reserved.
doi:10.1016/j.jpowsour.2008.12.008

Table 1
Syngas composition for four gasification processes from different companies [1].

	Air blown	British	Shell	Texaco
Component				
CO	15–30	54–57	62–65	45
H_2	18–25	29	28–30	30
CO_2	2–15	4.5	1.6–2	5–8
H_2O	3–11	[a]	0.4–2	18
N_2	45–55	[a]	0.7–3.1	0.8
Typical impurities (ppm)				
H_2S	750–7000	6000–7000	1260–4000	1100–3500
NH_3/HCN	50–500	[a]	300	800
HCl/HF	<50	[a]	200–830	170–690

[a] Not reported.

such as CeO_2, TiO_2, Al_2O_3, SiO_2 and, etc., showed catalytic activity in the various CO oxidation [26,27]. Recently, the unsupported Au catalysts were studied to determine their activity for CO oxidation [28]. Gold, present in a porous structure with nano-network, showed good catalytic activity for CO oxidation, showing that Au surface sites are catalytically active.

The recent innovative research has suggested that gold-based catalysts are potentially capable of being employed in fuel cells for CO oxidation [28–30]. The justification for developing the gold catalyst technologies is not only based on their promising technical performance, but also the price and availability of gold compared with the platinum group metals. Effectiveness of gold catalysts for CO conversion has already been demonstrated and showed preferential oxidation of carbon monoxide in hydrogen-rich gas [31,32]. However, the applications for gold in fuel cells so far are limited and include its use as sealant *O*-rings, corrosion resistant material and conductor to provide useful improvements in electrode conductivity [33,34].

The objective of this research is to examine the effectiveness of nano-Au catalyst supported on MoS_2 for the conversion of H_2 and CO in SOFC, by determining the fuel cell performances using this catalyst.

2. Experimental

2.1. Catalysts preparation

A two-stage method was used to prepare the Au/MoS_2 catalysts, comprising first the impregnation of MoS_2 with an acidic aqueous solution of $HAuCl_4$, followed by a washing step to remove chloride ions [35].

Impregnating was used to load Au particles (5 wt.%) onto the MoS_2 (Aldrich, 99.9%) surfaces. The stoichiometric amount of $HAuCl_4$ was dissolved in 1 L deionized water, and MoS_2 powder was added to the stirred solution. Then 10% aqueous ammonia was added dropwise at 5 mL min^{-1} with vigorous stirring until the pH was 11, after which the solution was stirred vigorously for a further 1 h. Next, the powders in the solution were separated by filtration and washed five times using deionized water to remove any chloride ions remaining on the surface, because chloride ions would deactivate the Au center and make the particles tend to sinter during the thermal pretreatment and catalytic operations [36].

2.2. Cell preparation

To prepare the anode materials, a mixture comprising Au/MoS_2 catalyst, 8% YSZ nano-powder (Inframat Advanced Materials) and silver powder (Alfa Aesar, 99.9%) in 85:5:10 weight ratio was dispersed in iso-propanol to make a suspension and intimately mixed in an ultrasonic bath for 1 h before drying by solvent evaporation to form a homogeneously mixed powder. The composite catalyst was so mixed to optimize the internal electrode configuration and maximize the triple phases boundary (TPB). Because MoS_2 itself is a semiconductor and its electronic conductivity is poor [37], 10 wt.% Ag powder was included in the composite anode to improve the electronic conductivity. To show the effect of nano-Au, another anode catalyst was made from the same MoS_2, YSZ and Ag using the same procedure, but containing no Au.

Dense pellets (2.54 cm in diameter and 0.3 mm in thickness) of 8 mol% YSZ (Intertec Southwest Inc.) were used as the electrolyte. Porous platinum was used as cathode catalyst, prepared by screen-printing platinum paste (Heraeus CL11-5100) on to one side of the YSZ pellets. After drying in air for 3 h, the Pt/YSZ pellet was further heated at 850 °C for 30 min to form porous cathodes. The anode materials were mixed with α-terpineol (Heraeus-372) to form viscous pastes that were screen printed on to the second side of the pellets and then dried by heating. The apparent anode surface area was 1 cm^2 and the anode thickness was approximately 0.15 mm.

Gold mesh welded to an Au lead wire was placed in intimate contact with the outer surfaces of each electrode. The YSZ electrolyte was secured between two coaxial alumina tubes, using ceramic sealant (Ceramabond 503, Aremcosame) around the rim on both sides of the electrolyte to seal the fuel cell compartments. The cell was heated in a tubular furnace (Thermolyne F79300) that could be operated at temperatures stable to ±0.1 °C within the fuel cell zone, while air and nitrogen flowed through the cathode and anode chambers, respectively. The fuel cell first was heated to 1000 °C to cure the sealant, then cooled down to a preselected operating temperature. After the operating temperature stabilized, the nitrogen stream was switched to fuel gas.

2.3. Electrochemical apparatus

In all tests, a Solartron Electrochemical interface (S1 1287) was used to monitor the open circuit voltage (OCV) between anode and cathode, measure electrochemical impedance and determine current–potential performance. Impedance data typically were obtained over the frequency range 1 MHz to 0.1 Hz. Potentiodynamic mode was used when performing current–potential measurements at a scanning rate of 5 mVs^{-1}. The cell was allowed to equilibrate and stabilize for at least 1 h after each change in operating conditions before conducting further measurements.

Gas analysis of the anode effluent streams was performed periodically during fuel cell experiments using gas chromatography (GC, HP5890).

3. Results and discussion

3.1. SEM images of the anode catalysts

Fig. 1 shows the backscattered images of the Au/MoS_2 catalyst. In the figure, Au appears as bright particles with various sizes. According to literature data [25,26], smaller Au particles have better catalytic activity for the conversion of CO.

To better estimate the Au particle size, higher resolution images were obtained using a field-emission scanning Auger microprobe (JAMP-9500F). Fig. 2 shows the catalyst's surface image. The Au particles were about 30–40 nm in diameter, the size reported to be catalytically active for the oxidation of CO [28].

3.2. Performances in CO-absent gas

MoS_2 showed catalytic activity for the conversion of H_2 and H_2S in SOFC in previous tests [23,37]. Here, the performances of Au/MoS_2 in the feed of H_2S-containing H_2, which has no CO, were compared first with those of MoS_2 alone. Fig. 3 shows the impedance measurements at 800 °C and 900 °C.

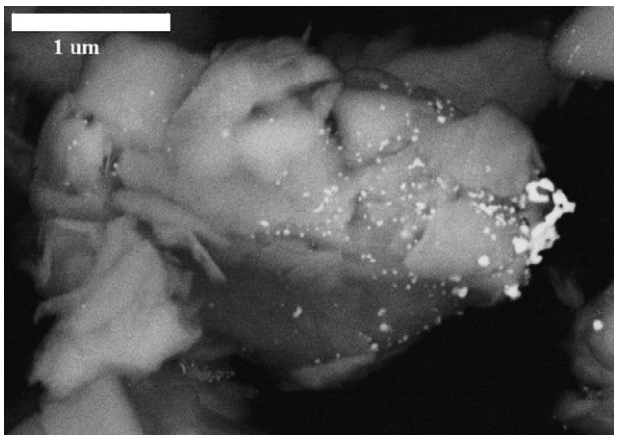

Fig. 1. SEM image of the Au/MoS_2 powders.

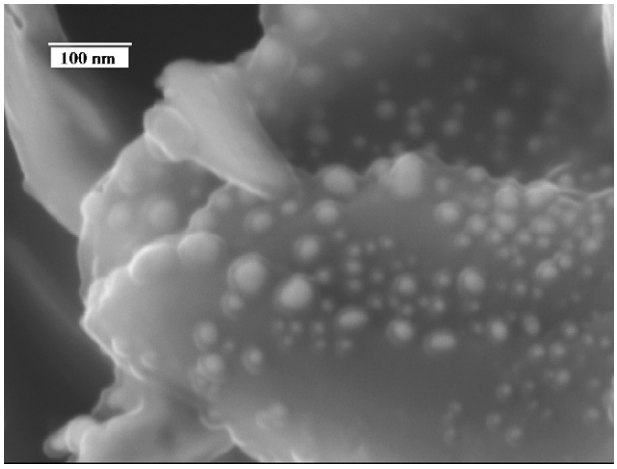

Fig. 2. SEM image of the Au/MoS_2 powders with higher magnification.

For each anode catalyst, the overall ohmic resistances decreased with increase in temperature, due to lower ohmic resistances of YSZ electrolyte and anode materials at higher temperature. However, the ohmic resistances for all the tests were still high. When the anode catalyst was MoS_2, the ohmic resistance values were about 8 Ω at 800 °C and 5 Ω at 900 °C. These high values are attributed to the low electronic conductivity of MoS_2, even when admixed with 10 wt.% Ag [37].

The polarization semicircle in the impedance spectra for Au/MoS_2 had slightly smaller radius than that for MoS_2 for each testing temperature (Fig. 3), which implied that Au/MoS_2 showed slightly improved activity for conversion of H_2 when compared with

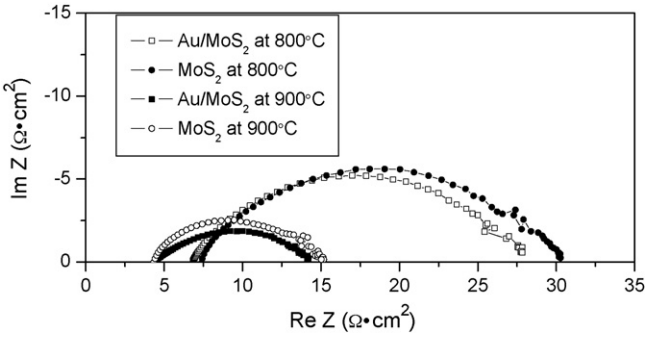

Fig. 3. Impedance spectra in $H_2 + H_2S$.

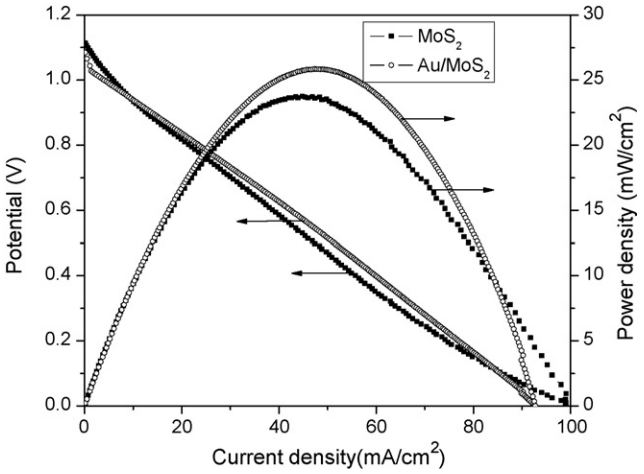

Fig. 4. IV-IP performances at 800 °C in $H_2 + H_2S$.

MoS_2 alone. As reported, nano-Au showed poor catalytic activity for the oxidation of H_2 or H_2S, but showed preferential activity for carbon monoxide in hydrogen-rich gas [31,32]. In SOFC, with the absence of CO in the feed gas, the inclusion of Au did not significantly improve the overall catalytic activity. The small radius for Au/MoS_2 was attributable to the improved contact between MoS_2 particles by the Au on the surface. Improved contact reduced the polarization radii for Au/MoS_2 when compared with MoS_2 at the same test temperatures.

Figs. 4 and 5 show the fuel cell performances with MoS_2 and Au/MoS_2 in H_2S-containing H_2 at 800 °C and 900 °C, respectively. Still, in the absence of CO, the fuel cell performances of supported Au/MoS_2 catalyst showed very limited improvement compared with MoS_2 alone at each testing temperature. The results were consistent with those from impedance spectra. It may be concluded that the nano-Au had poor catalytic activity for the conversion of H_2 or H_2S in SOFC.

For both catalysts, the discharging curves at 800 °C were almost straight lines, because of the high ohmic resistances of the fuel cells at this temperature (Fig. 4). Discharging curves can be divided into three parts corresponding to zones for activation loss, ohmic loss and concentration loss. At 800 °C the current–potential curve was characteristic of performance in which ohmic loss predominated, i.e. the impact of ohmic resistance was considerably higher than that of the activation resistance and mass transfer resistance. The ohmic resistance decreased from about 8 Ω to less than 5 Ω when

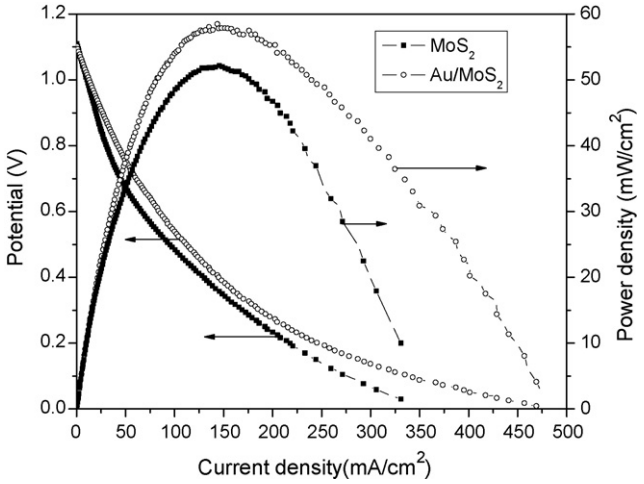

Fig. 5. IV-IP performances at 900 °C in $H_2 + H_2S$.

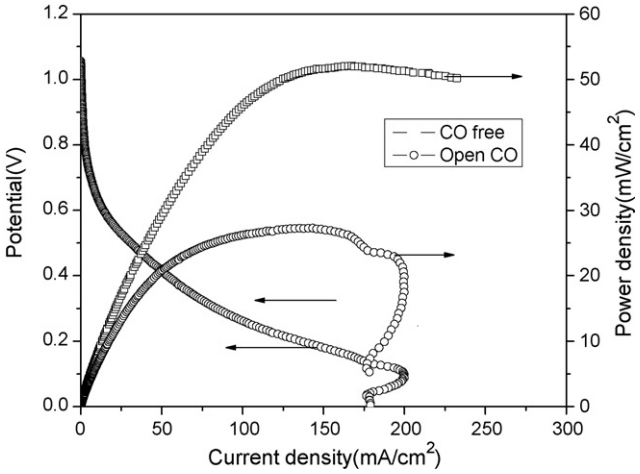

Fig. 6. IV-IP performances for MoS_2 alone in feed with and without CO at 900 °C.

the testing temperature reached 900 °C. At this temperature the ohmic losses had a lesser effect on the discharging curves, and the activation resistance was becoming more apparent.

3.3. Performances in CO-containing gas

For only MoS_2, CO would poison the catalyst. Figs. 6 and 7 show the performances and the impedance spectra, respectively, for MoS_2 alone at 900°C in the feed with and without CO. At the beginning of each test, only H_2 containing 5000 ppmv H_2S was fed into the anode compartment, then the feed was switched to H_2S-containing syngas (60% CO, 40% H_2 containing 5000 ppmv H_2S). The impedances and performances were measured both before and after the use of syngas to determine if there were changes in performance. Once the MoS_2 was exposed to CO in the syngas feed, the electrochemical polarization rapidly increased and the fuel cell performance dropped correspondingly. Thus, for only MoS_2 catalyst, the presence of CO in the feed gas poisoned the active sites.

Figs. 8 and 9 show the performances and impedance spectra, respectively, for Au/MoS_2 catalyst at 900°C using H_2S-containing syngas as a fuel. In the gas feed containing CO, the Au/MoS_2 catalyst showed improved performances relative to that in H_2S-containing H_2. This indicates preferential activity of nano-gold particles for oxidation of carbon monoxide.

The behavior of the Au/MoS_2 catalyst differed significantly from that of MoS_2 catalyst. When the catalyst is only MoS_2, CO would poison the catalyst, as described in previous section. Once the MoS_2 catalyst was exposed to CO, the electrochemical polarization rapidly increased and the fuel cell performance dropped correspondingly. In contrast, for the Au/MoS_2 anode catalyst, there was no poisoning effect from CO. In fact the performance was better when CO was present in the fuel. In Fig. 9, the impedance radius in CO-containing feed was smaller than that in CO-free feed. Thus, the polarization

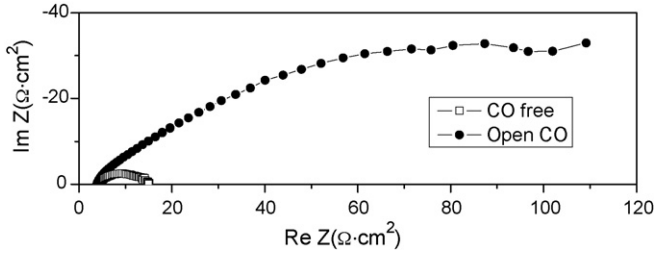

Fig. 7. Impedance spectra for MoS_2 alone in feed with and without CO at 900 °C.

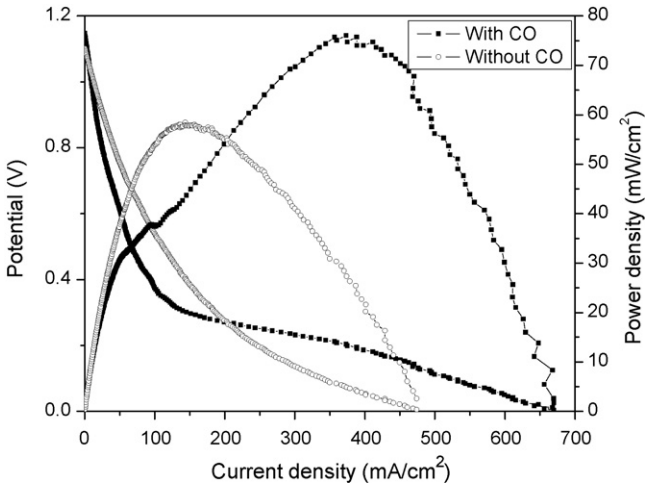

Fig. 8. IV-IP performances for Au/MoS_2 in feed gas with and without CO at 900 °C.

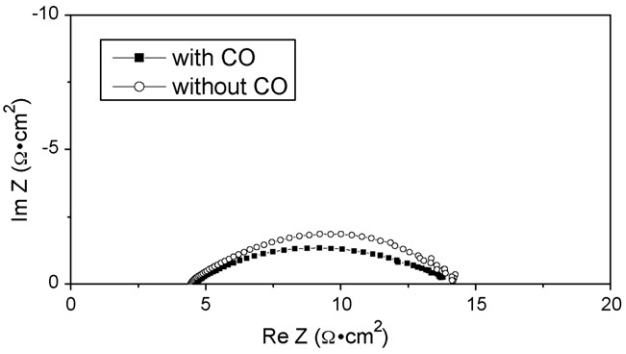

Fig. 9. Impedance spectra for Au/MoS_2 in feed gas with and without CO at 900 °C.

resistance for Au/MoS_2 catalyst decreased when CO was admixed into the feed. The maximum power density was 75 mW cm^{-2} in the CO-containing feed, compared with 58 mW cm^{-2} in the CO-free feed. The presence of supported nano-Au particles as Au/MoS_2 clearly reduced the polarization resistance and significantly improved the fuel cell performances when compared with MoS_2 alone in CO-containing gas feed. However, nano-gold particles tended to sinter at this temperature and led to degradation of fuel cell performance in long-term running. In next research, the sintering of nanoparticles will be studied; suitable spacer or support will be developed.

4. Conclusions

Au/MoS_2 is a promising anode catalyst for electrocatalytic oxidation of all components of H_2S-containing syngas in SOFC. The supported nano-Au particles have catalytic activity for CO oxidation in SOFC systems, thus preventing poisoning of MoS_2 active sites by CO. In contrast to use of MoS_2 as anode catalyst, performance of Au/MoS_2 anode catalyst improves when CO is present in the feed, which shows that the supported nano-Au is potentially useful catalyst for CO oxidation in fuel cell applications.

References

[1] A.T. Atimtay, D.P. Harrison, Ecol. Sci. 42 (1998) 163.
[2] M. Liu, P. He, J.L. Luo, A.R. Sanger, K.T. Chuang, J. Power Sources 94 (2001) 20–25.
[3] Y. Matsuzaki, I. Yasuda, Solid State Ionics 132 (2000) 261–269.
[4] G.A. Richards, D.A. Berry, A. Freed, J. Power Sources 134 (2004) 49–56.
[5] F.N. Cayan, M.J. Zhi, S.R. Pakalapati, I. Celik, N.Q. Wu, R. Gemmen, J. Power Sources 185 (2) (2008) 595–602.

[6] K.J. Liu, J.H. Luo, C. Johnson, X.B. Liu, J. Yang, S.X. Mao, J. Power Sources 183 (1) (2008) 247–252.
[7] Z.R. Xu, J.L. Luo, K.T. Chuang, A.R. Sanger, J. Phys. Chem. C 111 (44) (2007) 16679–16685.
[8] O. Costa-Nunes, R.J. Gorte, J.M. Vohs, J. Power Sources 141 (2005) 241–249.
[9] L. Aguilar, S. Zha, Z. Cheng, J. Winnick, M. Liu, J. Power Sources 135 (2004) 17–24.
[10] R. Mukundan, E.L. Brosha, F.H. Garzon, Electrochem. Solid State Lett. 7 (1) (2004) A5–A7.
[11] M. Liu, G.L. Wei, J.L. Luo, A.R. Sanger, K.T. Chuang, J. Electrochem. Soc. 150 (8) (2003) A1025–A1029.
[12] Y. Lu, L. Schaefer, J. Power Sources 135 (2004) 184–191.
[13] J.D. Oxley, M.M. Mdleleni, K.S. Suslick, Catal. Today 88 (2004) 139–151.
[14] M. Sun, A.E. Nelson, J. Adjaye, Catal. Today 105 (2005) 36–43.
[15] H. Farag, Energy Fuels 20 (5) (2006) 1815–1821.
[16] H. Acuna, R. Albiter, M.A. Espino, J. Ornelas, C. Alonso-Nunez, G. Paraguay-Delgado, F. Rico, J.L. Martinez-Sanchez, Appl. Catal. A: Gen. 304 (2006) 124–130.
[17] R. Prins, M. Egorova, A. Roethlisberger, Y. Zhao, N. Sivasankar, P. Kukula, Catal. Today 111 (1–2) (2006) 84–93.
[18] V. Vorontsov, W. An, J. Luo, K.T. S Chuang, Proceedings of the International Symposium on Fuel Cell and Hydrogen Technologies vol. 221, 1st, Calgary, AB, Canada, August 21–24, 2005.
[19] X.D. Wen, T. Zeng, Y.W. Li, J.G. Wang, H.J. Jiao, J. Phys. Chem. B 109 (39) (2005) 18491–18499.
[20] N. Arul Dhas, A. Ekhtiarzadeh, K.S. Suslick, J. Am. Chem. Soc. 123 (2001) 8310–8316.
[21] S.E. Skrabalak, K.S. Suslick, J. Am. Chem. Soc. 127 (2005) 9990–9991.
[22] W. Hyuk Suh, K.S. Suslick, J. Am. Chem. Soc. 127 (2005) 12007–12010.
[23] Z. Xu, J. Luo, K.T. Chuang, J. Electrochem. Soc. 154 (6) (2007) B523–B527.
[24] A.M. Venezia, G. Pantaleo, A. Longo, G.D. Carlo, M.P. Casaletto, F.L. Liotta, G. Deganello, J. Phys. Chem. B 109 (2005) 2821–2832.
[25] H.Y. Lin, Y.W. Chen, Ind. Eng. Chem. Res. 44 (2005) 4569–4576.
[26] W. Yan, S. Mahurin, B. Chen, S.H. Overbury, S. Dai, J. Phys. Chem. B 109 (2005) 15489–15496.
[27] D. Cameron, R. Holliday, D. Thompson, J. Power Sources 118 (2003) 298–303.
[28] C. Xu, J. Su, X. Xu, P. Liu, H. Zhao, F. Tian, Y. Ding, J. Am. Chem. Soc. 129 (1) (2007) 42–43.
[29] J.B. Xu, T.S. Zhao, Z.X. Liang, J. Power Sources 185 (2) (2008) 857–861.
[30] Y.W. Hen, M.H. Lin, H.C. Hsu, J.H. Lin, U.S. Pat. Appl. Publ. (2008), US2,008,241,038.
[31] Q. Elodie, M. Franck, D. Fabrice, A. Priscilla, C. Valerie, R. Jean-Luc, Appl. Catal. B: Environ. 80 (3–4) (2008) 195–201.
[32] R. Malgorzata, G. Barbara, L. Marek, W. Michal, Catal. Commun. 8 (8) (2007) 1284–1286.
[33] O.A. Marina, M. Mogensen, Appl. Catal. A 189 (1999) 117–126.
[34] C. Lu, W.L. Worrell, J.M. Vohs, R.J. Gorte, J. Electrochem. Soc. 150 (10) (2003) A1357.
[35] K. Mallick, M.J. Witcomb, M.S. Scurrell, J. Mol. Catal. A: Chem. 103 (2004) 215.
[36] Q. Xu, K. Kharas, A.K. Datye, Catal. Lett. 85 (2003) 229–235.
[37] M. Liu, G. Wei, J.L. Luo, A.R. Sanger, K.T. Chuang, J. Electrochem. Soc. 150 (8) (2003) A1025–A1029.